

Is depth perception of stereo plaids predicted by intersection of constraints, vector average or second-order feature?

Louise S. Delicato¹, Ning Qian*

*Center for Neurobiology and Behavior and Department of Physiology and Cellular Biophysics, Columbia University,
Kolb Annex Room 519, 1051 Riverside Drive, New York, NY 10032, United States*

Received 2 December 2003; received in revised form 22 April 2004

Abstract

Stereo plaid stimuli were created to investigate whether depth perception is determined by an intersection of constraints (IOC) or vector average (VA) operation on the Fourier components, or by the second-order (non-Fourier) feature in a pattern. We first created stereo plaid stimuli where IOC predicted vertical disparity, VA predicted positive diagonal disparity and the second-order feature predicted negative diagonal disparity. In a depth discrimination task, observers indicated whether they perceived the pattern as 'near' or 'far' relative to a zero-disparity aperture. Observers' perception was consistent with the disparity predicted by VA, indicating its dominance over IOC and the second-order feature in this condition. Additional stimuli in which VA predicted vertical disparity were created to investigate whether VA would dominate perception when it was a less reliable cue. In this case, observers' performance was consistent with disparity predicted by IOC or the second-order feature, not VA. Finally, in order to determine whether the second-order feature contributes to depth perception, stimuli were created where IOC and VA predicted positive horizontal disparity while the second-order feature predicted negative horizontal disparity. When the component gratings were oriented near horizontal ($\pm 83^\circ$ from vertical), depth perception corresponded to that predicted by the second-order feature. However, as the components moved away from horizontal ($\pm 75^\circ$ and $\pm 65^\circ$ from vertical), depth perception was increasingly likely to be predicted by an IOC or VA operation. These experiments suggest that the visual system does not rely exclusively on a single method for computing pattern disparity. Instead, it favours the most reliable method for a given condition.

© 2004 Elsevier Ltd. All rights reserved.

Keywords: Disparity; Non-Fourier; Second-order; Intersection of constraints; Vector average

1. Introduction

There is considerable research in the motion literature investigating how the visual system combines two (or more) one-dimensional (1D) motion vectors to form a two-dimensional (2D) pattern vector. However, there

has been little investigation of the same question in the case of depth from disparity. This paper seeks to redress this balance and investigates whether the visual system implements intersection of constraints (Adelson & Movshon, 1982; Albright, 1984; Fennema & Thompson, 1979; Movshon, Adelson, Gizzi, & Newsome, 1986) or vector average (Ferrera & Wilson, 1987; Wilson, Ferrera, & Yo, 1992; Wilson & Kim, 1994a, 1994b) operation on the Fourier components of stereo plaid stimuli. Furthermore, the extent to which the second-order (or non-Fourier) feature contributes to perception will also be investigated as there is extensive research indicating that it plays a significant role in depth and motion perception (Derrington, Badcock, & Holroyd,

* Corresponding author. Tel.: +1 212 543 6931x600; fax: +1 212 543 5816.

E-mail address: nq6@columbia.edu (N. Qian).

URL: <http://brahms.cpmc.columbia.edu>.

¹ Present address: School of Biology (Psychology), The Henry Wellcome Building for Neuroecology, University of Newcastle, Newcastle, Upon Tyne NE2 4HH, UK.

1992; Derrington & Ukkonen, 1999; Edwards, Pope, & Schor, 2000; Langley, Fleet, & Hibbard, 1999; McColl, Ziegler, & Hess, 2000; Wilcox & Hess, 1996; Wilcox & Hess, 1997).

The intersection of constraints (IOC) and vector average (VA) models are based upon a two-stage process. Each model suggests that the visual system decomposes a 2D pattern into its 1D Fourier components. The disparity or motion vector corresponding to each 1D component is computed (stage 1) and then combined according to some rule, IOC or VA (stage 2), to determine the 2D pattern disparity or motion. Any contribution of non-Fourier components into the VA computation is thought to be achieved by an additional parallel pathway (Wilson et al., 1992; Wilson & Kim, 1994a). In its present form the IOC does not take into consideration any non-Fourier input to the computation. Therefore, for simplicity, in the body of this paper we also consider a vector average of only the Fourier components and address the implications of including the second-order feature in VA computation in Section 7.

Stereo plaids have an advantage over moving plaids for determining which method (IOC, VA or second-order feature) the visual system employs. It has been shown that in depth discrimination tasks observers are considerably less sensitive to vertical disparities compared with horizontal disparities (Farell & Ahuja, 1996; Matthews, Meng, Xu, & Qian, 2003; Westheimer, 1984). This anisotropy can be exploited to distinguish between the different methods. In contrast, motion along the vertical and horizontal axes is perceived about equally well. The first experiment in this paper confirmed the disparity anisotropy with our experimental setup. We then conducted a series of experiments with similar stimuli to investigate the role of IOC,² VA or the second-order feature in depth perception. Our findings suggest that the visual system does not rely exclusively on a single method for combining 1D disparity signals; instead, it favours the most reliable cue for a given condition. Preliminary data have been reported in abstract form (Delicato & Qian, 2003).

2. General method

2.1. Apparatus

Stimuli were generated using an 8-bit ATI Rage 128 graphics card controlled by a G4 Apple Macintosh computer and presented on a 21" Viewsonic P225f monitor

with a resolution of 1024×768 and a refresh rate of 120 Hz. The mean luminance of the display was 49 cd/m^2 . A mirror stereoscope was used to present the left and right images to the left and right eyes respectively. Observers sat 75 cm from the display using a chinrest to stabilize head position and observations were made in a room lit only by the monitor.

2.2. Stimulus generation

Stimuli were generated in Matlab 5.2.1 using Video-Toolbox and Psychophysics Toolbox (Brainard, 1997; Pelli, 1997), and were saved beforehand. They were loaded in memory prior to the beginning of the experiment. The two half images of a stereogram were separated by 0.4° , and were presented on the central portion of the monitor. Each half image was $4.5^\circ \times 9^\circ$. A look-up-table was used to correct for the luminance non-linearity of the display.

2.3. Procedure

The method of constant stimuli was used in each experiment. The disparity range of the stimuli was chosen through trial and error in pilot studies to produce sufficiently complete psychometric curves for each observer in each condition. Experiments 1–3 used a single-interval forced-choice design. Prior to the start of each trial, observers fixated on a central fixation point and initiated the trial by pressing any button on the mouse. The fixation point was visible until the onset of the stimulus, where upon it disappeared. As soon as the stimulus finished, the fixation mark reappeared until the onset of the next stimulus. Observers' task was to indicate whether the pattern presented within the circular aperture appeared 'near' (left mouse button) or 'far' (right mouse button) with respect to a zero-disparity aperture surrounded by a zero-disparity plaid background (see each experiment for more details). Each stimulus was given an initial random phase to prevent observers from learning any monocular cue. All stimuli were pseudo-randomly presented such that no stimulus could be presented for the n th time until all stimuli had been presented $n - 1$ times. Stimuli were presented for 200 ms to minimise eye movement. Observers were given no feedback on their performance.

Experiment 4 used a temporal two-interval forced-choice design in which the patterns in the first and second intervals contained pattern disparities with opposite sign. Observers indicated whether the 'far' pattern appeared in the first (left mouse button) or second (right mouse button) temporal interval. All other aspects are as described above.

Sigmoidal psychometric curves were fitted with a logistic function of the form

² It should be noted that the disparity or motion vector of the high contrast intersections of plaid stimuli (blobs) is indistinguishable from IOC. Therefore, any results about IOC are equally applicable to the blobs.

$$f(x) = \gamma + (1 - \gamma - \lambda) \frac{1}{1 + \exp[-(x - \alpha)/\beta]},$$

using the `psignifit` package (<http://bootstrap-software.org/psignifit/>), which implements the maximum-likelihood method described by Wichmann & Hill (2001). The particular fitting function is not important in this study; the different rules for determining pattern disparity can be differentiated according to whether the slopes of the curves are positive, negative, or nearly flat.

2.4. Observers

Three observers participated in the study, one of whom was completely naive to the aims. All observers had normal or corrected to normal vision and could correctly respond to the Randot™ stereo test at 20 s of arc (viewing distance of 40 cm).

2.5. Second-order features

It is thought that second-order features are generated in the visual system by a non-linear operation on the Fourier components of stimuli. Here we consider the effect of the lowest-order non-linearity, squaring, on a plaid (Derrington, 1987; Scott-Samuel & Georgeson, 1999; Wilson et al., 1992).

A plaid is the sum of two differently oriented sinusoidal gratings, and its luminance profile can be expressed as:

$$I(x, y) = I_1[1 + c_1 \cos(\vec{\omega}_1 \cdot \vec{x} + \phi_1)] + I_2[1 + c_2 \cos(\vec{\omega}_2 \cdot \vec{x} + \phi_2)].$$

Here $\vec{\omega}_n$ ($n = 1, 2$) are the angular spatial frequency vectors for the two gratings, and are defined as $\vec{\omega}_n = 2\pi(u_n, v_n)$ with u_n and v_n being the horizontal and vertical spatial frequencies of the gratings, respectively. Each $\vec{\omega}_n$ so defined is perpendicular to the orientation of the corresponding grating. $\vec{x} = (x, y)$ is the positional vector, and I_n , c_n , and ϕ_n are the mean luminances, contrasts, and phases of the gratings, respectively.

Squaring the above expression produces the following four second-order terms in addition to the original grating components $c_1 \cos(\vec{\omega}_1 \cdot \vec{x} + \phi_1)$ and $c_2 \cos(\vec{\omega}_2 \cdot \vec{x} + \phi_2)$:

$$c_1^2 \cos(2\vec{\omega}_1 \cdot \vec{x} + 2\phi_1), \quad (1)$$

$$c_2^2 \cos(2\vec{\omega}_2 \cdot \vec{x} + 2\phi_2), \quad (2)$$

$$c_1 c_2 \cos[(\vec{\omega}_1 + \vec{\omega}_2) \cdot \vec{x} + (\phi_1 + \phi_2)], \quad (3)$$

$$c_1 c_2 \cos[(\vec{\omega}_1 - \vec{\omega}_2) \cdot \vec{x} + (\phi_1 - \phi_2)], \quad (4)$$

For convenience we define:

$$\vec{\omega}_+ = \vec{\omega}_1 + \vec{\omega}_2,$$

$$\vec{\omega}_- = \vec{\omega}_1 - \vec{\omega}_2.$$

Therefore, the second-order features have frequency vectors that are double the original gratings ($2\vec{\omega}_1$ and $2\vec{\omega}_2$; expressions (1) and (2) respectively), or are the sum ($\vec{\omega}_+$; expression (3)) or difference ($\vec{\omega}_-$; expression (4)) of the original gratings. For the parameters used in this study, the feature with the lowest frequency is the most salient perceptually (see Fig. 1). Therefore, if the visual system were to compute pattern disparity based upon a second-order feature, the lowest spatial frequency feature is the most likely candidate. It is proposed that the higher frequency second-order terms are removed by low-pass filtering in the brain (Wilson et al., 1992).³ Further discussion on the second-order features in this paper will focus on the lowest frequency feature.

Since $\vec{\omega}_1$ and $\vec{\omega}_2$ always have the same magnitude ω in our experiments (i.e., the two gratings always have the same spatial-frequency magnitude), the four second-order features have frequency magnitudes of 2ω , 2ω , $\omega_+ = 2\omega \cos(\theta/2)$, and $\omega_- = 2\omega \sin(\theta/2)$, respectively, where θ is the angle between $\vec{\omega}_1$ and $\vec{\omega}_2$ and is equal to the difference in orientation between the two gratings. If θ is less than 90° , the lowest frequency second-order feature corresponds to the difference feature; however, if θ is greater than 90° it corresponds to the sum feature. In addition, the sum and the difference features have orthogonal orientations (i.e., $\vec{\omega}_+$ and $\vec{\omega}_-$ are perpendicular to each other) when $\vec{\omega}_1$ and $\vec{\omega}_2$ have the same magnitude.

There is an inherent ambiguity in the definition of the direction of the $\vec{\omega}_n$ ($n = 1$ or 2). For a given grating orientation, $\vec{\omega}_n$ could point in either one of the two opposite directions, orthogonal to the orientation. Therefore, with two gratings in a plaid, there are four possible combinations, as shown in Fig. 2. The angle (θ) between $\vec{\omega}_1$ and $\vec{\omega}_2$ in the top two choices differs from that in the bottom two choices by 90° . Therefore, if the lowest frequency second-order feature corresponds to the difference feature under the top two choices, it will correspond to the sum feature under the bottom two choices. In addition, for a given grating, changing the direction of $\vec{\omega}_n$ will change the sign of ϕ_n . The results, however, will not be affected by the choice as long as a single definition is used consistently. For convenience, we always choose θ to be less than 90° so that the difference feature is always the lowest frequency feature.

³ Since the effect of a fixed low-pass filter depends on the actual frequencies of the features, an adaptive low-pass filter may have to be assumed to always preserve the lowest-frequency feature.

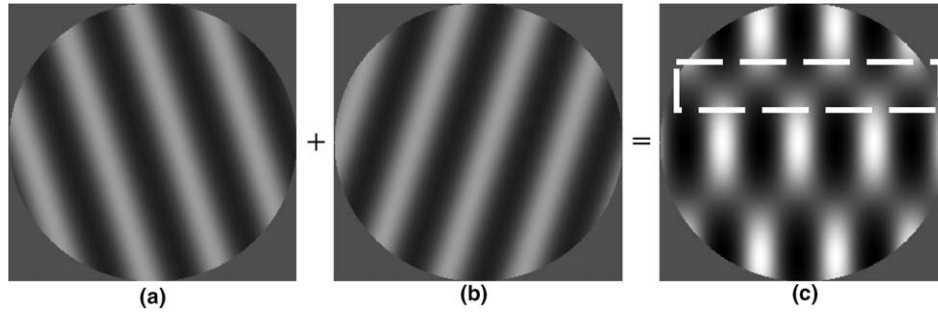


Fig. 1. When two differently oriented 1D sinusoidal gratings (panels a and b) are summed they form a 2D plaid (panel c). The gratings shown are oriented at $\pm 17.5^\circ$ from vertical, respectively. The lowest frequency second-order feature of the plaid is also periodic but oriented horizontally, and only a part of it is marked by a dashed horizontal rectangle in panel c.

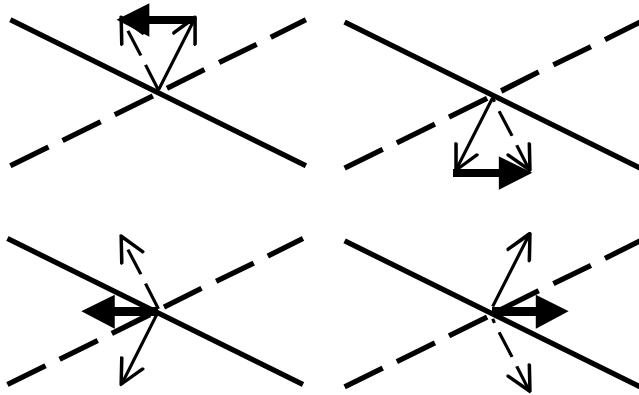


Fig. 2. Ambiguity in choosing the angular frequency vector $\vec{\omega}_n$. The two grating orientations are represented by the long solid and dashed lines, respectively. For each of the two grating orientations, the corresponding spatial frequency vector (the thin solid or dashed arrows) can take either one of the two opposite directions perpendicular to the orientation, resulting in a total of four possible choices shown here. The frequency vector for the lowest frequency second-order feature (bold solid arrow) in each case is also shown. In the top two cases where the angle, θ , between the two component frequency-vectors is smaller than 90° , the difference second-order feature is the lowest frequency feature. In the bottom two cases, θ is larger than 90° , and the sum feature is the lowest frequency feature. The results in the paper do not depend on the choice of $\vec{\omega}_n$, and for convenience we will always let the angle be less than 90° so that the difference feature is the lowest frequency second-order feature. One should not confuse the frequency vectors with the disparity vectors which are not ambiguous.

2.6. Plaid disparity according to VA, IOC, or second-order feature

The equations we used for calculating the pattern disparity of the plaid based on VA, IOC, or the lowest frequency second-order feature are listed here.⁴

2.6.1. VA

The VA expression is straightforward:

⁴ For all mathematical derivations, angles are measured counter-clockwise from the horizontal axis. However, we often describe angles from vertical for ease of discussion in the rest of the paper.

$$\vec{D}_{VA} = (\vec{D}_1 + \vec{D}_2)/2, \quad (5)$$

where \vec{D}_1 and \vec{D}_2 , are the disparity vectors of the two component gratings. These vectors are perpendicular to the corresponding grating orientations by virtue of the aperture problem, and are therefore parallel to $\vec{\omega}_1$ and $\vec{\omega}_2$, respectively.

2.6.2. IOC

By considering the projections of the IOC vector onto the two constraint lines, one can readily obtain two equations whose solution gives the horizontal and vertical components of IOC disparity as:

$$D_{IOC,x} = \frac{D_1 \sin \theta_2 - D_2 \sin \theta_1}{\sin(\theta_2 - \theta_1)},$$

$$D_{IOC,y} = \frac{D_1 \cos \theta_2 - D_2 \cos \theta_1}{\sin(\theta_1 - \theta_2)},$$

where D_n is the magnitude and θ_n the direction (counter-clockwise from horizontal axis) of the disparity of the Fourier components. Equivalently, the total magnitude and direction of the IOC disparity are:

$$D_{IOC} = \sqrt{D_{IOC,x}^2 + D_{IOC,y}^2}, \quad (6)$$

$$\theta_{IOC} = \tan^{-1} \frac{D_{IOC,y}}{D_{IOC,x}}. \quad (7)$$

In the case where the disparity of one grating component in the plaid is 0 and the other is D , the IOC direction is parallel to the orientation of the zero-disparity grating and the expression for the IOC magnitude reduces to:

$$D_{IOC} = D / \sin \theta,$$

where θ is the angle between the two grating orientations.

2.6.3. Second-order feature

The expressions for the second-order feature disparities are derived in [Appendix A](#). For the special case where the two grating components have the same

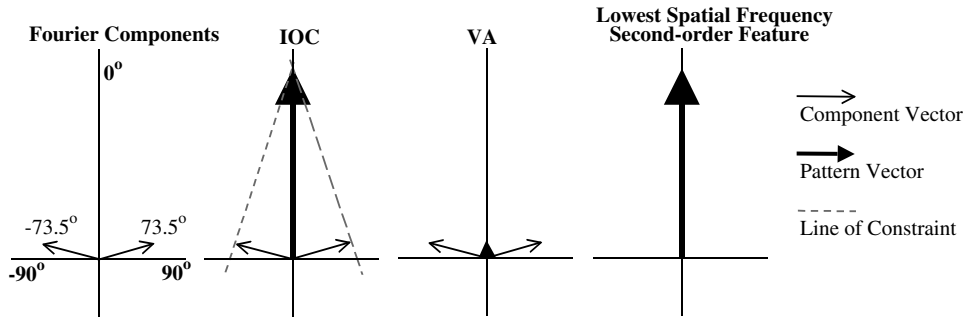


Fig. 3. The disparity vectors in Experiment 1. In the example shown here, the plaid was composed of two gratings oriented at $\pm 17.5^\circ$ from vertical, and the disparity vectors of the Fourier components (thin arrows) were in the directions of $\pm 73.5^\circ$ from vertical (left panel). This resulted in vertical disparities of IOC, VA and the lowest frequency second-order feature as indicated by the bold arrows in the right three panels, respectively. The second-order feature was oriented horizontally as shown in Fig. 1. Patterns with horizontal disparities were generated by rotating everything in this figure by 90° .

frequency magnitude, the disparity magnitude and direction of the difference second-order feature are:

$$D_{2\text{nd}}^- = (D_1 - D_2) / [2 \sin(\theta/2)], \quad (8)$$

$$\alpha_- = (\alpha_1 - \alpha_2) / 2, \quad (9)$$

with α_1 and α_2 being the directions of $\vec{\omega}_1$ and $\vec{\omega}_2$ respectively. Here D_n ($n = 1$ or 2) is positive if it is in the same direction of $\vec{\omega}_n$ and negative if it is in the opposite direction.

Since we will choose to let θ be less than 90° (Fig. 2), the difference feature is also the lowest frequency feature.

3. Experiment 1

Previous research has shown that in depth discrimination tasks, observers are usually much less sensitive to vertical than to horizontal disparity (Farell & Ahuja, 1996; Matthews et al., 2003; Westheimer, 1984). There are, however, special cases where depth perception from vertical and horizontal disparity is equally strong (Backus, Banks, van Ee, Crowell, & Crowell, 1999).⁵ Therefore, Experiment 1 seeks to confirm the disparity anisotropy under our experimental condition. Stimulus parameters in this and subsequent experiments were chosen to generate coherent stimuli. Observers never reported perceiving more than one depth signal in any stimulus; they always perceived a coherent plaid pattern.

Observers were presented with two stimulus conditions. In one condition the plaid stimuli contained only vertical disparity (Fig. 3). The stimuli were composed of two sinusoidal gratings oriented at $\pm 17.5^\circ$ from vertical on a plaid background composed of gratings oriented at

$\pm 17.5^\circ$ from horizontal. In the other condition the plaid stimuli contained only horizontal disparity, and the stimuli were identical to the vertical disparity condition except that all components were rotated by 90° . All stimuli contained component gratings with a contrast of 0.5, a spatial frequency of $1.5c^\circ$, and were presented within a 3° circular aperture on a $4.5^\circ \times 9^\circ$ plaid background for 200 ms.⁶ Disparity was symmetrically introduced to the two gratings such that the plaid disparity was in a vertical or horizontal direction. Under such conditions, the disparity predictions of the IOC, VA and the lowest frequency second-order feature all have the same direction (see Fig. 3). The disparity ranges were different for each individual observer. In the following, when we refer to the disparity of a plaid stimulus without qualification, we mean the pattern, instead of the component, disparity.

3.1. Results

Fig. 4 shows the performance of three observers discriminating whether the stereo plaid stimuli appeared ‘near’ or ‘far’ with respect to the zero-disparity aperture. The percentage of times observers perceived the pattern as ‘near’ is plotted as a function of the disparity of the Fourier components. For stimuli with a large negative or positive horizontal disparity, observers perceived the patterns as ‘near’ or ‘far’ on $\sim 100\%$ of trials, respectively. All observers showed some bias when reporting their perception of zero-disparity stimuli; these patterns were more likely to be perceived as ‘near’.⁷ For stimuli

⁵ Note that Backus et al. (1999) measured the effect of varying the vertical size ratio on estimates of slant; the vertical size ratio generates a gradient of vertical disparity whereas this paper uses constant vertical disparities.

⁶ A plaid (pattern) background was selected because informal observations suggested that the plaid background aided observers’ ability to perform the depth discrimination compared with a uniform mean luminance background.

⁷ A possible explanation is that observers might consider the plaid within the circular aperture to be ‘figure’ and the rectangular plaid background to be ‘ground’, and thus more likely respond to the zero-disparity stimuli as ‘near’.

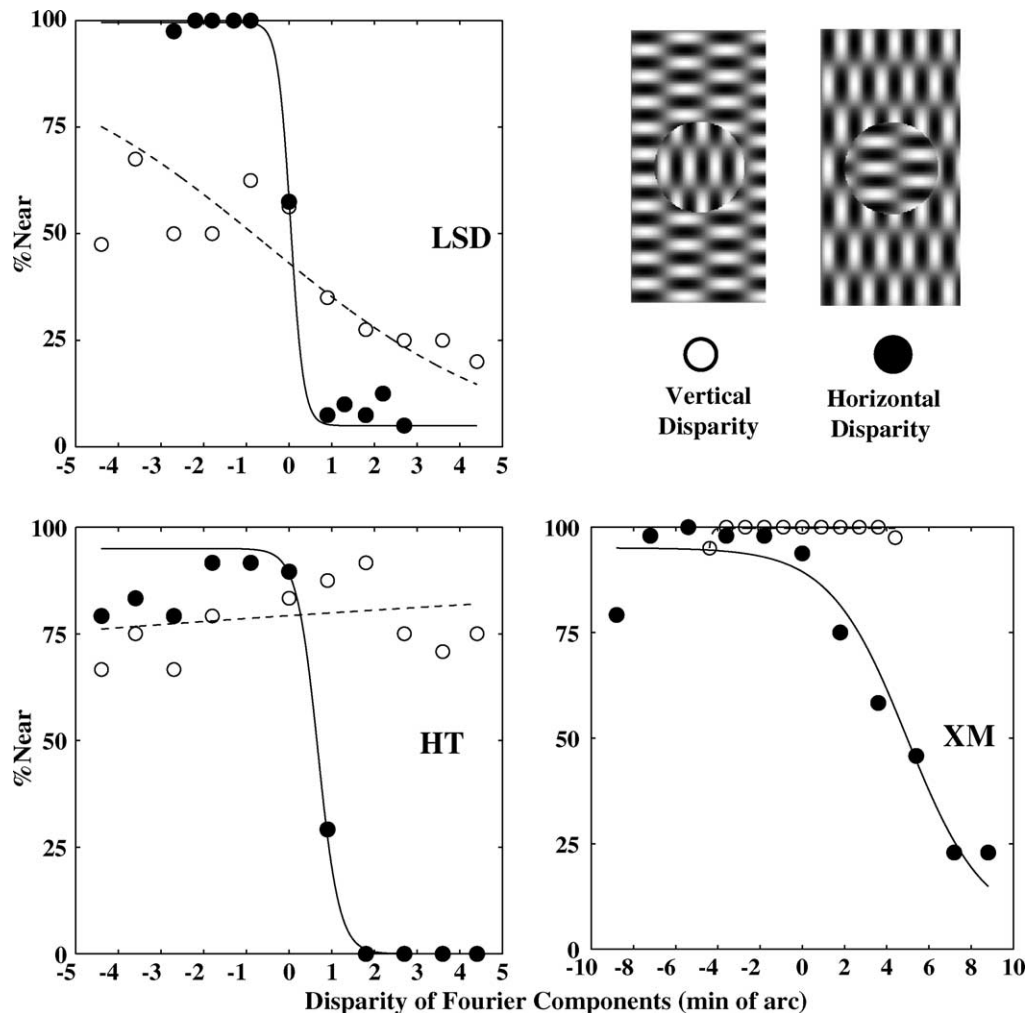


Fig. 4. The results from Experiment 1 for three observers. The percentage of trials in which observers perceived the pattern as 'near' is plotted as a function of the disparity of each Fourier component in the stimulus. The data for the horizontal plaid disparity are represented by filled dots and fitted with solid curves. Those for the vertical plaid disparity are represented by open dots and fitted with dashed curves. There are 40 observations per point for each observer. Note that observer XM required larger stimulus disparity than the other observers to perform the task.

that contained only a vertical disparity, depth discrimination was more difficult as the curves are flat for two observers (XM and HT). Although there was some depth discrimination for observer LSD, performance was markedly reduced in this condition compared with the horizontal disparity condition. Note that as the stimuli did not have vertical magnification, observers never reported perceiving the stimuli as being rotated about a vertical axis.

The above result confirms that depth discrimination is considerably poorer with vertical disparity than with horizontal disparity under our experimental condition. Indeed, since the small, multi-orientation plaids used here do not satisfy the optimal conditions for depth perception from vertical disparity (Matthews et al., 2003), the depth assignment of the vertical-disparity stimuli appears arbitrary. This is desirable for our purpose as the large difference between vertical and horizontal disparities will facilitate the differentiation of IOC, VA, and the

second-order feature for computing plaid disparity; if a particular rule predicts a vertical disparity but the psychometric curve is normal, we know immediately that the rule is not used.

It should be noted that the depth discrimination task used in this experiment differs from the disparity-detection task in which observers have to distinguish a zero-disparity plaid from non-zero ones regardless of their perceived depths. It has been shown that observers have no difficulty with detection of vertical disparity (Farell, 2003).

4. Experiment 2

To test whether the visual system uses IOC, VA, or the second-order feature, stimuli were devised such that each of these methods predicted different disparity directions. Stereo plaid stimuli containing two sinusoidal

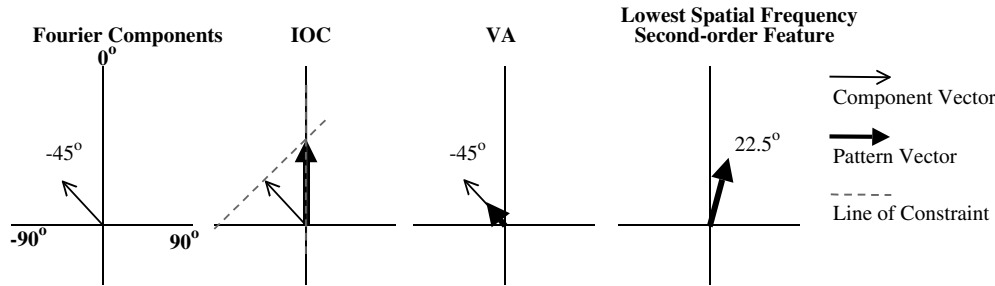


Fig. 5. The disparity vectors in Experiment 2. The plaids were composed of a zero-disparity grating oriented at 0° and a grating with variable disparity oriented at 45° or -45° (from vertical). The example here shows the case of 45° orientation of the variable-disparity component whose disparity vector was -45° from vertical (left panel). The predicted disparities according to IOC, VA, and the second-order feature are shown as bold arrows in the right three panels, respectively. The format of presentation is identical to that of Fig. 3.

components were created where one vertically oriented grating (0°) had zero disparity while the disparity of the other, diagonally oriented grating ($\pm 45^\circ$ from vertical; Fig. 5) varied. As a control, we also created single grating stimuli oriented at $\pm 45^\circ$; this condition illustrates the performance expected if VA was employed. In each condition (plaid or grating) the data from both diagonal cases (+ and -45°) were pooled together. All other stimulus details were as Experiment 1.

Under these conditions, the plaid disparity according to IOC was always vertical, while the disparities according to VA and the second-order feature have horizontal components with opposite signs. Fig. 5 shows an example where IOC predicts upward vertical disparity, VA predicts disparity on the left side of vertical, and the second-order feature predicts disparity on the right side of vertical (see equations in Section 2.6). Each of these methods has a different prediction:

1. If the visual system implements IOC only, then depth discrimination would be expected to be extremely difficult (see Experiment 1). In this case the psychometric function would have a relatively flat slope.
2. If the visual system implements VA, then depth perception of the plaid would be consistent with that of the corresponding grating control. In this case the psychometric function would have a negative slope (the same as the grating condition).
3. As the horizontal-disparity sign of the second-order feature is opposite to that predicted by VA, if the visual system uses this feature to discriminate depth, perception would be the *opposite* of that predicted by VA. In this case the psychometric function would have a positive slope.

4.1. Results

In Fig. 6, the percentage of times observers perceived a stimulus as ‘near’ with respect to the zero-disparity aperture is plotted as a function of the disparity of the Fourier component. Observers perceived the grating

control as ‘near’ when it had a large negative disparity and ‘far’ when it had a large positive disparity (open symbols), as expected. When observers were presented with the plaid pattern (filled symbols), the psychometric function has the same sign as that of the grating condition. Therefore, the results are consistent with the visual system using VA. As previously, observers were biased towards perceiving zero-disparity stimuli as ‘near’.⁷

This experiment demonstrates that under these stimulus conditions, the visual system does not rely on IOC or the second-order feature to extract depth from disparity.

However, it is possible that VA was used only as a consequence of the difficulty in recovering depth with IOC because IOC predicted vertical disparity. This issue is addressed in the next experiment.

5. Experiment 3

Stimuli were created where VA predicted only vertical disparity while IOC and the second-order feature predicted disparity with both a vertical and horizontal component (see Fig. 7). The stimuli were identical to those in Experiment 2 except that they have been rotated by 45° clockwise or counterclockwise to make VA along vertical axis. All other aspects of the experiment were the same as Experiment 2.

In this experiment IOC and the second-order feature predicted disparity with a horizontal and vertical component that had the same sign. Therefore, if a good psychometric function is obtained we do not know whether this results from an implementation of the IOC or the second-order feature. However, if VA were used by the visual system to perform the depth discrimination, as indicated by Experiment 2, then observers’ performance would be poor (see Experiment 1).

5.1. Results

Fig. 8 shows the percentage of times observers perceived a stimulus as ‘near’ with respect to the

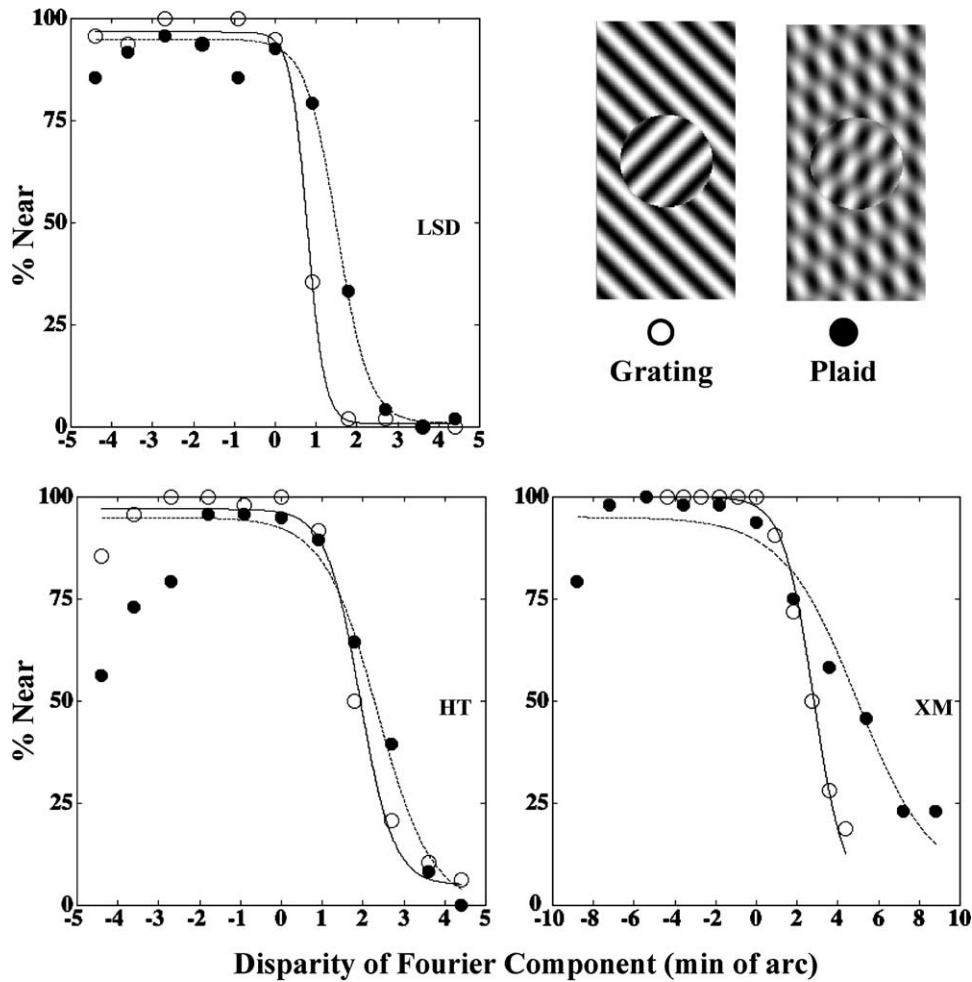


Fig. 6. The results from Experiment 2 for three observers. The percentage of trials in which observers perceived the pattern as ‘near’ is plotted as a function of the disparity of the Fourier component. There are two stimulus conditions, plaid and grating (see text). The data for the plaid condition are represented by filled dots and fitted with solid curves, while those for the grating condition were represented by open dots and fitted with dashed curves. There are 40 observations per point for observers LSD and HT, and 48 observations per point for observer XM. Note that observer XM required larger stimulus disparity than the other observers to perform the task.

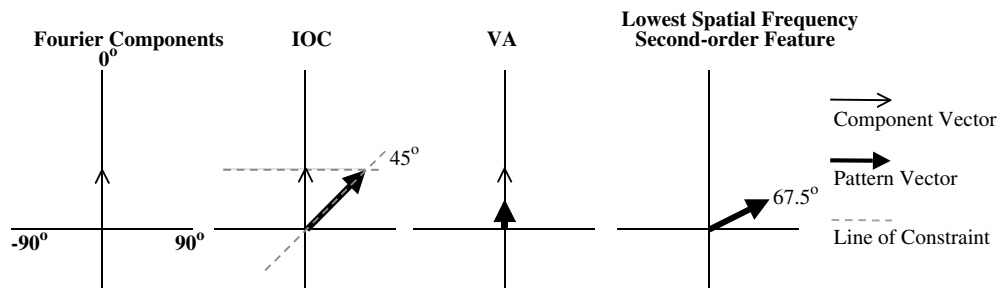


Fig. 7. The disparity vectors in Experiment 3. The vectors are as Fig. 5 (Experiment 2) except that here everything has been rotated by 45° such that the VA disparity is vertical.

zero-disparity aperture as a function of the disparity of the Fourier component. At large negative disparity, observers perceived the pattern as ‘far’, and at large positive disparity observers perceived the pattern as ‘near’.

As with the previous experiments, there was a tendency for observers to perceive zero-disparity stimuli as ‘near’.⁷ The results obtained are consistent with the visual system using IOC or the second-order feature to ex-

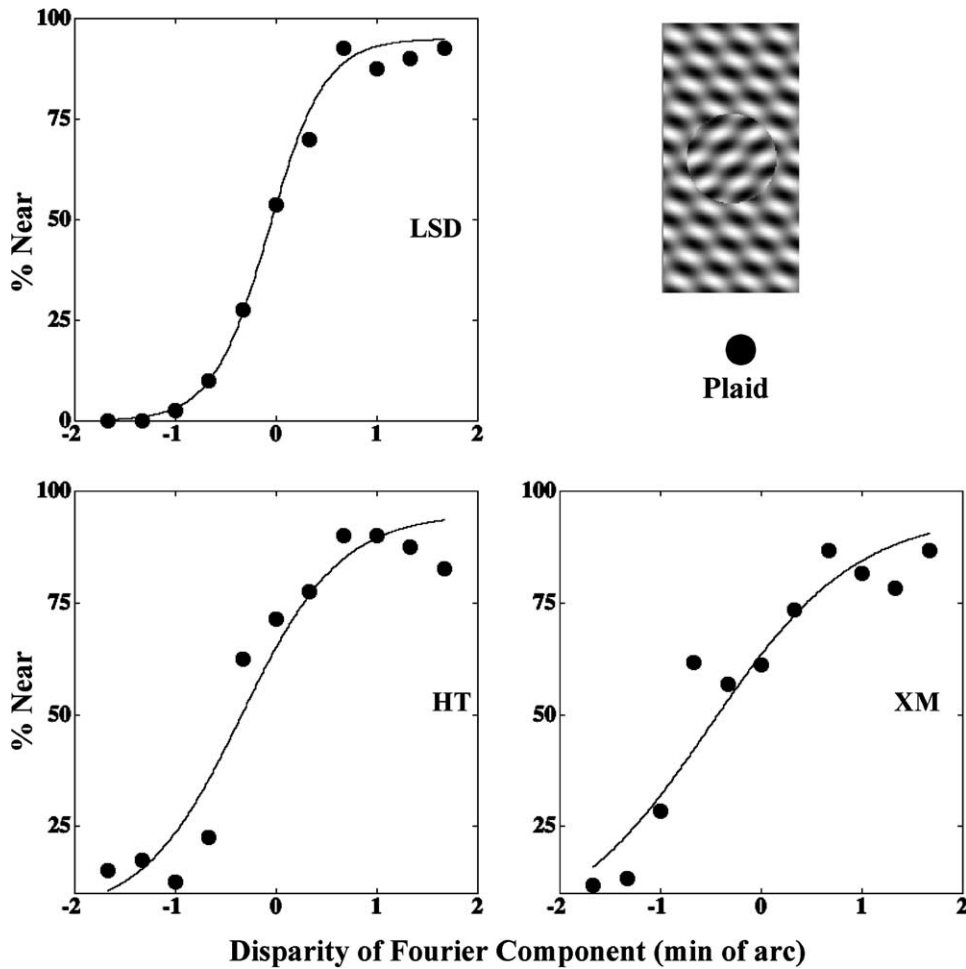


Fig. 8. The results from Experiment 3 for three observers. The percentage of trials in which observers perceived the pattern as 'near' is plotted as a function of the disparity of the Fourier component. There are 40 observations per point for observers LSD and HT and 50 observations per point for observer XM.

tract depth from disparity, and are not consistent with the disparity predicted by VA. This, in combination with the previous experiment, suggests the following:

1. The visual system has more than one method available to recover depth from disparity and it does not rely on one method exclusively.
2. Depth perception is determined by the most sensitive mechanism (the one that predicts a horizontal disparity component).

Thus far it is not clear what role, if any, the second-order feature plays in depth perception. Therefore, in Experiment 4 stimuli were devised whereby a computation based upon the Fourier components (IOC or VA) or the second-order feature each predicted horizontal disparity but with opposite sign. This experiment may create more evenly matched alternatives to the visual system as each method predicts horizontal disparity.

6. Experiment 4

Derrington et al. (1992) showed that both Fourier and non-Fourier components play a role in the perceived direction of motion of plaids (see also Derrington & Ukkonen, 1999). In a periodic stimulus, such as a grating or plaid, the perceived direction of a shift depends on the size of the shift. If the shift size is less than half of the period of the pattern, the perceived direction of motion agrees with the direction of the shift. However, if the shift is greater than half of the stimulus period and less than one period, the perceived direction of motion is *opposite* to the direction of the shift. Derrington et al., showed that when the Fourier components in a plaid, comprised of two sinusoidal gratings with equal spatial frequency, were shifted $3/8$ of their period (or $3\pi/4$ phase shift), the lowest spatial frequency second-order feature shifted $3/4$ of its period, or equivalently $1/4$ in the opposite direction (see Appendix A for a detailed mathematical analysis). Under this stimulus condition, a pattern is produced whereby IOC or VA of the Fourier

components predicts rightwards motion, say, while the second-order feature predicts leftwards motion. The authors found that when both component orientations were less than about 70° from vertical, IOC or VA of the Fourier components predicted the perceived direction of motion of the plaid; otherwise, the perceived direction of motion of the plaid was consistent with that predicted by the second-order feature.⁸

Such plaid patterns can be used to determine whether the visual system uses Fourier components or the second-order feature to recover depth from disparity in conditions where each method predicts horizontal disparity but with opposite sign. Therefore, whether the observer perceives a stimulus as ‘near’ or ‘far’ at varying shifts in the phase disparity of the Fourier components will show whether the visual system uses the Fourier components (either IOC or VA) or the second-order feature (non-Fourier component).

Three sets of plaid stimuli were created by superimposing two sinusoidal gratings with orientations of $\pm 83^\circ$, $\pm 75^\circ$, and $\pm 65^\circ$ (from vertical), respectively. The spatial frequency of each grating component was 3.1 c/° . The phase shifts of the two grating components were identical in magnitude but opposite in sign, and varied between 0° and 360° in steps of 22.5° . The disparity corresponding to IOC, VA and the second-order feature varied with the orientation of the Fourier components as well as phase shift. All other stimulus details are as Experiment 1. All orientations of the component gratings were more than 45° away from vertical to ensure that the disparity of the lowest frequency second-order feature is horizontal.

Fig. 9 shows the disparity predicted by IOC, VA and the second-order feature plotted as a function of the phase disparity of the Fourier components. It takes into account the fact that the phase disparity of the second-order feature is twice as large as that of each grating component (see Appendix A), and that when the disparity of any periodic pattern is greater than half cycle, the perceived disparity is in the opposite direction to the actual shift (to be referred to as reversal hereafter). From this we can make the following predictions:

1. If the visual system uses the Fourier components to recover depth (IOC or VA), depth discrimination performance plotted as a function of the phase disparity of the Fourier components in the plaid is expected to contain only one peak. This peak will lie between phase disparities of 0° and 180° and the trough between phase disparities of 180° and 360° (see Fig. 9).

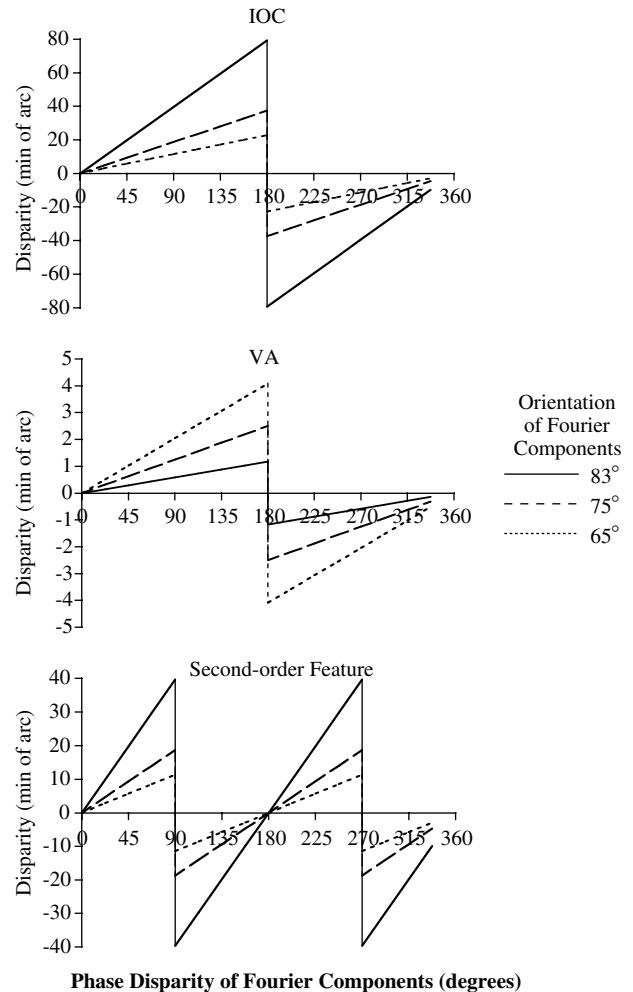


Fig. 9. The horizontal disparities in Experiment 4 predicted by IOC, VA and the second-order feature are plotted as a function of the phase disparity of the Fourier components in the pattern. The results for component grating orientations of $\pm 83^\circ$, $\pm 75^\circ$, and $\pm 65^\circ$ from vertical are shown as solid, dashed, and dotted curves, respectively. Note that (i) due to the sign reversal, the magnitude of the disparity of IOC is considerably greater than that of the second-order feature over the domain of 90° – 270° , and both disparities are greater than that of VA, (ii) the magnitude of IOC and the second-order feature increases as the orientation of the Fourier components become further away from vertical, while the disparity of VA decreases as the orientation of the Fourier components become further away from vertical, and (iii) the disparity of the second-order feature cycles twice within a single cycle of the Fourier components, while the IOC and VA cycle once.

2. If the visual system uses the second-order feature to recover depth then it is expected that there will be two peaks in observers’ psychometric curves. One peak will lie between phase disparities of 0° and 90° (trough between 90° and 180°) and the other between phase disparities 180° and 270° (trough between 270° and 360° , see Fig. 9).

Note that under the stimulus conditions of this experiment, were it not for the disparity reversal, the IOC and the second-order feature would have predicted exactly

⁸ It should be noted that the periodicity of the intersection blobs follows that of the Fourier components instead of the second-order feature.

the same disparity values (see proof in Appendix A). Also note that the disparity predicted by IOC and the second-order feature decreases, while the disparity predicted by VA increases, as the orientation of the components moves away from horizontal.

6.1. Results

In a temporal two-interval forced-choice depth discrimination task observers indicated whether the ‘far’ stimulus appeared in the first or second interval. Fig. 10 shows the percentage of times observers perceived the plaid as ‘far’ (relative to its opposite disparity reference in the same trial) plotted as a function of the phase disparity of the Fourier components. Since all three observers showed a similar trend, each curve in Fig. 10 shows the mean data (± 1 s.e.m). When the components were oriented at $\pm 83^\circ$ (from vertical) there are two clear peaks in the function. This indicates that the second-order feature dominated observers’ perception. As the orientation of the components moved closer to vertical

($\approx 75^\circ$ from vertical) the peaks in the function became less prominent, indicating that depth perception became increasingly dependent upon the Fourier components and less dependent upon the second-order feature. Furthermore, when the components were oriented at $\pm 65^\circ$ (from vertical) the psychometric function contained only one peak indicating that depth perception was dominated by an operation on the Fourier components (IOC or VA).

The results show that when the VA or IOC of the Fourier components and the second-order feature both predict horizontal disparity, there are other contributing factors that determine the method used to recover depth (e.g., the orientation of the Fourier components). Similar orientation dependency was found by Derrington et al. (1992) in motion perception. The orientation dependency could be interpreted in terms of cue reliability. Specifically, when the orientation of the component gratings is close to horizontal, the horizontal disparity they carry may become less reliable (Chen & Qian, 2004; Farell, 2003), and the visual system may thus ‘choose’ to use

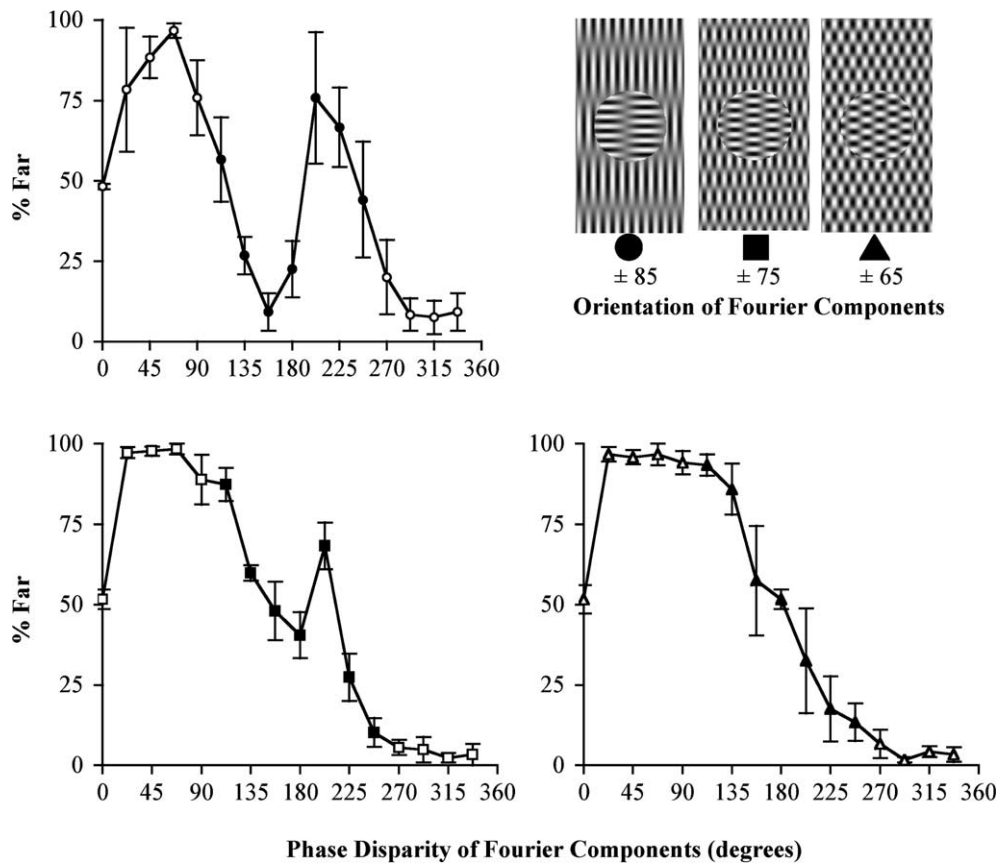


Fig. 10. The results from Experiment 4. The percentage of trials in which observers perceived the plaid as ‘far’ (relative to its opposite-disparity reference in the same trial) is plotted as a function of the phase disparity of the Fourier components (degrees). The graphs represent the mean data from three observers plus and minus 1 s.e.m. The plaid was comprised of components oriented at $\pm 83^\circ$ (circle), $\pm 75^\circ$ (square), or $\pm 65^\circ$ (triangle) from vertical as indicated in the upper right corner. Filled symbols represent phases where the Fourier components and second-order features predict disparity with opposite sign. Each observer made 40 observations per point under each condition.

the horizontal disparity carried by the vertically oriented second-order feature.

7. Discussion

By exploiting the difference in depth discrimination between vertical and horizontal disparities (Experiment 1), stereo plaid stimuli were created for determining the contribution of IOC, VA and the second-order feature to compute the pattern disparity. Experiments 2 and 3 showed that the visual system rejected whatever method predicted vertical disparity, in favour of one which predicted disparity with a horizontal component. When stimulus conditions were such that the Fourier components and the second-order feature each predicted horizontal disparity, but with opposite sign, the method employed by the visual system was dependent upon the orientation of the Fourier components (Experiment 4). These experiments demonstrate that the visual system does not rely exclusively on a single method for computing pattern disparity for depth perception, but instead favours the most reliable cue under a given condition (Landy, Maloney, Johnston, & Young, 1995).

It is important to note that in all of the experiments presented in this paper, observers never reported perceiving the plaid pattern as incoherent (i.e., one of the gratings in the plaid pattern was perceived as lying on a different depth plane than the other). The patterns were always perceived as a coherent plaid on one depth plane. Indeed if it were the case that the plaids in Experiment 3 were perceived incoherently, observers' depth perception would have been poor as the only grating component with a disparity in that stimulus predicted vertical disparity.

Some discussion is required to address the issue of whether or not the second-order feature in a pattern should be included in a vector average computation as is the case with the model proposed by Wilson et al. (1992). In our study the vector average computation was computed based on the Fourier components alone. This is not an issue in Experiment 1 as IOC, VA, and the second-order feature all predicted the same disparity direction and the purpose there was to establish the difference between vertical and horizontal disparities. In Experiment 4, the second-order disparity was much larger than VA disparity (Fig. 9). Therefore, if the second-order feature is included in the averaging, VA will be dominated by the second-order feature with two peaks in Fig. 9. The conclusion will remain essentially the same that the visual system uses the second-order feature when the component orientations are close to horizontal and IOC otherwise. The issue becomes important in Experiment 3 where IOC and VA with the second-order feature included make indistinguishable predictions.

However, Experiment 2 suggests that the second-order feature really should not be included in VA, at least for the patterns used in this paper. The reason is that VA *with* the second-order feature and VA *without* the second-order feature will predict opposite horizontal-disparity signs, and the results in Fig. 6 are only consistent with the latter.

We argued that in Experiment 4, the reason why the Fourier components predict depth perception at orientations closer to vertical ($\pm 65^\circ$ from vertical) and not at those further away from vertical ($\pm 83^\circ$ from vertical) is that the horizontal disparity of the Fourier components becomes less reliable as their orientations are closer to horizontal (Chen & Qian, 2004; Farell, 2003). An alternative explanation suggested by Fig. 9 is that when the components are oriented at $\pm 83^\circ$ (from vertical), IOC disparity may be too large and VA disparity too small, while the second-order disparity may be closest to optimal magnitude. This is also consistent with the notion that the visual system uses the most reliable disparity cue for a given condition. Further investigation is needed for determining which interpretation is more appropriate.

Our experiments only show clear evidence for the use of VA and second-order feature but not IOC. Specifically, Experiment 2 found evidence for VA; Experiment 3 found evidence for either IOC or second-order feature but could not distinguish between them; Experiment 4 found evidence for IOC or VA (but again could not distinguish them) at some grating orientations, and second-order feature at other orientations. To establish the role of IOC, a plaid in which the IOC vector is considerably away from the VA and second-order vectors, instead of between them or parallel to one of them, would be needed. We have not been able to create such a plaid. On the other hand, current data cannot rule out IOC either, and further studies would be needed to clarify the issue.

Farell (1998) created two plaid conditions in which the gratings in the plaids had the same horizontal-disparity sign, but the grating intersections (blobs/IOC) had the opposite horizontal-disparity sign. He found that the plaids were perceived to have opposite depth, as predicted by the blobs. However, the perception may also be driven by the lowest spatial frequency second-order feature, the feature investigated in this paper, as this feature had the same horizontal-disparity sign as the blobs. Using an adaptation paradigm Farell argues against this idea. He found that adaptation only influenced perception when the adapting stimulus was parallel to the grating components, not when it was parallel to the blobs or the second-order feature. Farell argues that the visual system computes 2D pattern disparity by a two-stage process in which the disparity of each Fourier component is computed and combined to determine the disparity of the blobs. He concluded that the

second-order feature does not play a role in computing 2D pattern disparity.

However, this conclusion may need to be revised in light of the work of Langley et al. (1999) who suggest that the site of adaptation is prior to the non-linearity required to process the second-order stimuli. It is possible that in Farell's study, the null effect of adaptation, when the adapting stimulus was matched to the second-order feature, occurred as a consequence of the site of adaptation being prior to the non-linearity. Therefore, Farell's result may also be consistent with the hypothesis that the visual system used the disparity of the second-order feature to perceive depth.

Weiss, Simoncelli, & Adelson (2002) have developed a Bayesian model to predict the perceived velocity of translating patterns by considering measurement noises and a prior preference to slow motion. They show that a considerable amount of psychophysical data, that was previously accounted for by either IOC, VA or feature-tracking, can be explained by their model (Bowns, 1996; Burke & Wenderoth, 1993; Stone, Watson, & Mulligan, 1990; Thompson, 1982; Yo & Wilson, 1992). In particular, the model can explain that at high contrast the perceived direction of a plaid is consistent with IOC while at low contrast the perceived direction is predicted by VA.

However, one should be cautious when considering a VA explanation of perceived motion at low contrast. Research has shown that at low contrast, plaid patterns tend not to be perceived to move as a single coherent pattern; rather, the components of the pattern are perceived to move incoherently over one another (Delicato & Derrington, 2001). Therefore, if observers were required to indicate the direction of motion of a pattern that was actually incoherent due to the low contrast, the average of their responses over many trials would be indistinguishable from the direction of motion predicted by VA.

While Weiss et al., did not consider any psychophysical data pertaining to depth perception from disparity, there is a possibility that motion and disparity may be processed by a common mechanism (Qian & Andersen, 1997; Qian, Andersen, & Adelson, 1994). It would therefore be interesting to examine whether a similar model, incorporating the disparity predicted by the second-order feature, could account for the depth perception data presented here.

Acknowledgments

We thank Drs. Vincent Ferrera, Xin Meng, Hirokazu Tanaka, and two anonymous reviewers for their very helpful comments. This work was supported by NIH grant MH 54125 and a McDonnell Foundation grant.

Appendix A. Derivation of the second-order feature disparities

The left and right eyes' luminance patterns can each be represented as a sum of two gratings:

$$I_l(x, y) = I_1[1 + c_1 \cos(\vec{\omega}_1 \cdot \vec{x} + \phi_{1l})] \\ + I_2[1 + c_2 \cos(\vec{\omega}_2 \cdot \vec{x} + \phi_{2l})],$$

$$I_r(x, y) = I_1[1 + c_1 \cos(\vec{\omega}_1 \cdot \vec{x} + \phi_{1r})] \\ + I_2[1 + c_2 \cos(\vec{\omega}_2 \cdot \vec{x} + \phi_{2r})],$$

where ϕ_{ne} ($n = 1, 2; e = l, r$) is the phase of the n th grating in eye e . The two gratings thus have phase disparities of $\Delta\phi_1 = \phi_{1l} - \phi_{1r}$ and $\Delta\phi_2 = \phi_{2l} - \phi_{2r}$, respectively.

The disparities of all second-order features can be calculated as follows. First, according to expressions (1)–(4) in Section 2.5, the disparity vectors for the four second-order features are parallel to the directions of $\vec{\omega}_1, \vec{\omega}_2, \vec{\omega}_+$ and $\vec{\omega}_-$, respectively. Second, to determine their amplitudes, we need to compare the expressions for the left and right eyes corresponding to each second-order term.⁹ It is easy to see from expressions (1)–(4) that the phase disparities of the four second-order features are:

$$(\Delta\phi)_{2nd}^1 = 2\Delta\phi_1,$$

$$(\Delta\phi)_{2nd}^2 = 2\Delta\phi_2,$$

$$(\Delta\phi)_{2nd}^+ = \Delta\phi_1 + \Delta\phi_2,$$

$$(\Delta\phi)_{2nd}^- = \Delta\phi_1 - \Delta\phi_2,$$

respectively.

For any periodic pattern, when the phase disparity $\Delta\phi$ is larger than π and less than 2π , it is effectively a phase disparity of opposite sign given by $\Delta\phi - 2\pi$. For the special case of $\Delta\phi_2 = -\Delta\phi_1$ in Experiment 4, when the component gratings' phase disparities vary from 0 to 2π , the phase disparity of the difference feature (as well as the two frequency doubled features) will vary from 0 to 4π . Therefore, as the gratings' phase disparity increases in magnitude from 0 to 2π , there will be one sign inversion for the grating disparity and for the VA and IOC operations on the grating disparity, but two sign inversions for the disparity of the difference second-order feature (Fig. 9). Consequently, there will be circumstances where VA and IOC of the grating components predict a disparity of one sign, while the second-order feature predicts a disparity of the opposite sign. For example, if $\Delta\phi_1 = -\Delta\phi_2 = 3\pi/4$, generating a positive horizontal disparity according to VA or IOC, then

⁹ An implicit assumption in the above derivation is that the non-linearity for generating the second-order features occurs prior to binocular combination (Wilcox & Hess, 1996).

$(\Delta\phi)_{2nd}^- = 3\pi/2$ which is effectively $-\pi/2$, a negative horizontal disparity for the second-order feature.

For any periodic pattern with angular spatial frequency ω , its phase disparity $\Delta\phi$ is related to the ordinary disparity D (expressed in visual angle) according to $\Delta\phi = \omega D$. Therefore, according to expressions (1)–(4) in the text, the ordinary disparities of the four second-order features are:

$$D_{2nd}^1 = (2\phi_{1l} - 2\phi_{1r}) / |2\vec{\omega}_1| = \Delta\phi_1 / \omega_1 = D_1,$$

$$D_{2nd}^2 = (2\phi_{2l} - 2\phi_{2r}) / |2\vec{\omega}_2| = \Delta\phi_2 / \omega_2 = D_2,$$

$$\begin{aligned} D_{2nd}^+ &= [(\phi_{1l} - \phi_{1r}) + (\phi_{2l} - \phi_{2r})] / |\vec{\omega}_+| \\ &= (\Delta\phi_1 + \Delta\phi_2) / |\vec{\omega}_+| \\ &= (\omega_1 D_1 + \omega_2 D_2) / |\vec{\omega}_1 + \vec{\omega}_2|, \end{aligned}$$

$$\begin{aligned} D_{2nd}^- &= [(\phi_{1l} - \phi_{1r}) - (\phi_{2l} - \phi_{2r})] / |\vec{\omega}_-| \\ &= (\Delta\phi_1 - \Delta\phi_2) / |\vec{\omega}_-| \\ &= (\omega_1 D_1 - \omega_2 D_2) / |\vec{\omega}_1 - \vec{\omega}_2|, \end{aligned}$$

respectively.

If $\omega_1 = \omega_2 = \omega$, as is the case for all the experiments reported here, the above results can be reduced to:

$$D_{2nd}^1 = D_1,$$

$$D_{2nd}^2 = D_2,$$

$$D_{2nd}^+ = (D_1 + D_2) / [2 \cos(\theta/2)],$$

$$D_{2nd}^- = (D_1 - D_2) / [2 \sin(\theta/2)]$$

where θ is the angle between $\vec{\omega}_1$ and $\vec{\omega}_2$.

One can further decompose these disparities into their horizontal and vertical components. Assume that the directions of $\vec{\omega}_1$ and $\vec{\omega}_2$ are α_1 and α_2 , counterclockwise from the horizontal axis, then, the direction of $\vec{\omega}_+$ will be $\alpha_+ = (\alpha_1 + \alpha_2)/2$, and direction of $\vec{\omega}_-$ will be $\alpha_- = (\alpha_1 - \alpha_2)/2$. The horizontal and vertical components of D_{2nd}^n are simply $D_{2nd}^n \cos \alpha_n$ and $D_{2nd}^n \sin \alpha_n$ for $n = 1, 2, +$ and $-$. Note that α_n ($n = 1$ or 2) differs from the corresponding grating orientation θ_n ($n = 1$ or 2) by 90° .

For the special case of $\omega_1 = \omega_2 = \omega$, there is a simple relation between the IOC disparity and the disparities of the sum and difference second-order features: The projections of the IOC disparity along the $\vec{\omega}_+$ and $\vec{\omega}_-$ directions are exactly equal to D_{2nd}^+ and D_{2nd}^- . In other words, if the disparity vectors for the sum and difference features are added vectorially, the result is equal to the IOC vector. To demonstrate, note that the projections of \vec{D}_{IOC} in the directions of $\vec{\omega}_1$ and $\vec{\omega}_2$ are simply D_1 and D_2 respectively (cf Fig. 3):

$$(\vec{\omega}_1 / \omega) \vec{D}_{IOC} = D_1,$$

$$(\vec{\omega}_2 / \omega) \vec{D}_{IOC} = D_2$$

Add and subtract the two equations, we have:

$$(\vec{\omega}_+ / \omega) \vec{D}_{IOC} = D_1 + D_2,$$

$$(\vec{\omega}_- / \omega) \vec{D}_{IOC} = D_1 - D_2$$

where $\vec{\omega}_+$ and $\vec{\omega}_-$ are the directions of the sum and difference second-order disparities, and are perpendicular to each other when $\omega_1 = \omega_2 = \omega$. Therefore, the projections of \vec{D}_{IOC} along the these two orthogonal directions are:

$$D_{IOC}^+ = (D_1 + D_2) / [2 \cos(\theta/2)],$$

$$D_{IOC}^- = (D_1 - D_2) / [2 \sin(\theta/2)]$$

which equal to D_{2nd}^+ and D_{2nd}^- respectively. This completes the proof.

Since $D_{2nd}^+ = 0$ in Experiment 4, this result explains why D_{2nd}^- would be equal to D_{IOC} in Fig. 9 were it not for the different number of sign reversals for the two cases. D_{2nd}^+ is also equal to 0 in Experiment 1, and since the disparities in Experiment 1 are too small to trigger sign reversal, D_{2nd}^- does equal to D_{IOC} (Fig. 3).

References

- Adelson, E. H., & Movshon, J. A. (1982). Phenomenal coherence of moving visual-patterns. *Nature*, 300(5892), 523–525.
- Albright, T. D. (1984). Direction and orientation selectivity of neurons in visual area MT of the Macaque. *Journal of Neurophysiology*, 52, 1106–1130.
- Backus, B. T., Banks, M. S., van Ee, R., Crowell, J. A., & Crowell, D. (1999). Horizontal and vertical disparity, eye position, and stereoscopic slant perception. *Vision Research*, 39(6), 1143–1170.
- Bowns, L. (1996). Evidence for a feature tracking explanation of why type II plaids move in the vector sum direction at short durations. *Vision Research*, 36(22), 3685–3694.
- Brainard, D. H. (1997). The psychophysics toolbox. *Spatial Vision*, 10(4), 433–436.
- Burke, D., & Wenderoth, P. (1993). The effect of interactions between one-dimensional component gratings on two-dimensional motion perception. *Vision Research*, 33(3), 343–350.
- Chen, Y., & Qian, N. (2004). A coarse-to-fine disparity energy model with both phase-shift and position-shift receptive field mechanisms. *Neural Computation*, 16, 1545–1577.
- Delicato, L. S., & Derrington, A. M. (2001). Low contrast plaids are incoherent. *Investigative Ophthalmology and Visual Science*, 42(4), S737–S737.
- Delicato, L. S., & Qian, N. (2003). Is depth perception of stereo plaids predicted by intersection of constraints, vector average or second-order features? [Abstract]. *Journal of Vision*, 3(9), 97a.
- Derrington, A. M. (1987). Distortion products in geniculate X-cells—a physiological-basis for masking by spatially modulated gratings. *Vision Research*, 27(8), 1377–1386.
- Derrington, A. M., Badcock, D. R., & Holroyd, S. A. (1992). Analysis of the motion of 2-dimensional patterns: evidence for a second-order process. *Vision Research*, 32(4), 699–707.
- Derrington, A. M., & Ukkonen, O. I. (1999). Second-order motion discrimination by feature-tracking. *Vision Research*, 39(8), 1465–1475.
- Edwards, M., Pope, D. R., & Schor, C. M. (2000). First- and second-order processing in transient stereopsis. *Vision Research*, 40(19), 2645–2651.

- Farell, B. (1998). Two-dimensional matches from one-dimensional stimulus components in human stereopsis. *Nature*, 395(6703), 689–693.
- Farell, B. (2003). Detecting disparity in two-dimensional patterns. *Vision Research*, 43(9), 1009–1026.
- Farell, B., & Ahuja, S. (1996). Binocular disparities of 1-D and 2-D contours. *Investigative Ophthalmology and Visual Science*, 37(3), 1307–1307.
- Fennema, C. L., & Thompson, W. B. (1979). Velocity determination in scenes containing several moving objects. *Computer Graphics and Image Processing*, 9, 301–315.
- Ferrera, V. P., & Wilson, H. R. (1987). Direction specific masking and the analysis of motion in two dimensions. *Vision Research*, 27(10), 1783–1796.
- Landy, M. S., Maloney, L. T., Johnston, E. B., & Young, M. (1995). Measurement and modeling of depth cue combination: in defense of weak fusion. *Vision Research*, 35(3), 389–412.
- Langley, K., Fleet, D. J., & Hibbard, P. B. (1999). Stereopsis from contrast envelopes. *Vision Research*, 39(14), 2313–2324.
- Matthews, N., Meng, X., Xu, P., & Qian, N. (2003). A physiological theory of depth perception from vertical disparity. *Vision Research*, 43(1), 85–99.
- McColl, S. L., Ziegler, L., & Hess, R. F. (2000). Stereodeficient subjects demonstrate nonlinear stereopsis. *Vision Research*, 40(9), 1167–1177.
- Movshon, J. A., Adelson, E. H., Gizzi, M. S., & Newsome, W. H. (1986). The analysis of moving visual patterns. In C. Chagas, R. Gatass, & C. Gross (Eds.), *Pattern Recognition Mechanisms* (pp. 117–151). New York: Springer.
- Pelli, D. G. (1997). The VideoToolbox software for visual psychophysics: transforming numbers into movies. *Spatial Vision*, 10(4), 437–442.
- Qian, N., & Andersen, R. A. (1997). A physiological model for motion-stereo integration and a unified explanation of Pulfrich-like phenomena. *Vision Research*, 37(12), 1683–1698.
- Qian, N., Andersen, R. A., & Adelson, E. H. (1994). Transparent motion perception as detection of unbalanced motion signals. 1. Psychophysics. *Journal of Neuroscience*, 14(12), 7357–7366.
- Scott-Samuel, N. E., & Georgeson, M. A. (1999). Does early non-linearity account for second-order motion. *Vision Research*, 39(17), 2853–2865.
- Stone, L. S., Watson, A. B., & Mulligan, J. B. (1990). Effect of contrast on the perceived direction of a moving plaid. *Vision Research*, 30(7), 1049–1067.
- Thompson, P. (1982). Perceived rate of movement depends on contrast. *Vision Research*, 22(3), 377–380.
- Weiss, Y., Simoncelli, E. P., & Adelson, E. H. (2002). Motion illusions as optimal percepts. *Nature Neuroscience*, 5(6), 598–604.
- Westheimer, G. (1984). Sensitivity for vertical retinal image differences. *Nature*, 307(5952), 632–634.
- Wichmann, F. A., & Hill, N. J. (2001). The psychometric function: I. Fitting, sampling and goodness-of-fit. *Perception and Psychophysics*, 63(8), 1293–1313.
- Wilcox, L. M., & Hess, R. F. (1996). Is the site of nonlinear filtering in stereopsis before or after binocular combination? *Vision Research*, 35(4), 1490–1490.
- Wilcox, L. M., & Hess, R. F. (1997). Scale selection for second-order (non-linear) stereopsis. *Vision Research*, 37(21), 2981–2992.
- Wilson, H. R., Ferrera, V. P., & Yo, C. (1992). A psychophysically motivated model for two-dimensional motion perception. *Visual Neuroscience*, 9(1), 79–97.
- Wilson, H. R., & Kim, J. (1994a). A model for motion coherence and transparency. *Visual Neuroscience*, 11(6), 1205–1220.
- Wilson, H. R., & Kim, J. (1994b). Perceived motion in the vector sum direction. *Vision Research*, 34(14), 1835–1842.
- Yo, C., & Wilson, H. R. (1992). Perceived direction of moving two-dimensional patterns depends on duration, contrast and eccentricity. *Vision Research*, 32(1), 135–147.